

COUPLING A NETWORK HVAC MODEL TO A COMPUTATIONAL FLUID DYNAMICS MODEL USING LARGE EDDY SIMULATION

Jason Floyd

Hughes Associates, Inc
3610 Commerce Dr #817
Baltimore, MD 21227 USA
e-mail: jfloyd@haifire.com

ABSTRACT

An HVAC network model was coupled to FDS v5.5. The HVAC model allows a user to specify the topology of an HVAC system along with dampers, fans, and forward/reverse flow loss through ducts and fittings. The model was indirectly coupled with the FDS flow solver. The HVAC model uses prior time step values as its boundary conditions and provides to FDS wall boundary conditions of temperature, velocity, and species for prediction of the next FDS time step. The current implementation does not account for transport times with the HVAC network. This paper describes the governing equations for the HVAC network model which is based upon the MELCOR, a nodal network model used for nuclear power plant containment buildings, solver. The specific numerical implementation of the equations within FDS is described.

A series of verification exercises demonstrate that the network model correctly models HVAC flows and that its coupling with FDS maintains mass conservation. A simple and a complex validation exercise show that the combined solvers can accurately predict HVAC flows for a duct network in a complex geometry with fire effects

INTRODUCTION

In the built environment, fire protection engineers have been limited in their ability to model large structures. Two-zone models (e.g. CFAST (Jones, 2009)) and air quality models (e.g. CONTAM (Walton, 2008)) allow one to model an entire building and include the effects of mechanical ventilation systems. Neither class of model, however, is in itself an adequate solution. Zone models have generally limited ability to model HVAC (heating, ventilating, and air conditioning) systems and air quality models do not contain all the necessary physics to model the effects of a fire. One-zone models providing both a high level of HVAC capability along with the ability to model fire effects have been developed (Floyd, 2004), but as with any lumped parameter method, one cannot obtain detailed solutions in regions of interest such as the room of origin.

CFD (computational fluid dynamics) models can provide a very high level of detail, but modeling HVAC systems in a CFD model is a difficult task. Grid resolutions to accurately predict flow and pressure loss within a duct network would make gridding a duct network unaffordable for most CFD users. Even if it were affordable, a significant validation effort would be required to demonstrate that reasonable predictions of pressure loss were being made.

Recent FDS (McGrattan, 2010) development has greatly improved the stability of FDS when using multiple computational meshes and added the capability to compute pressure rises on a room-by-room basis. This added capability means that one could take a large structure and grid some regions very coarsely (where detailed resolution is not needed) and some regions finely and have an affordable whole building computation. However, FDS v5.5 contains only rudimentary HVAC capabilities. One can specify inlet and outlet flows, but one cannot couple inlets to outlets. Additionally there is no manner in which pressurization effects, flow losses, or other HVAC related phenomena can be addressed.

A solution to this is to couple an HVAC network model to the CFD model. This concept was proposed by Schaelin (1993) and a variety of efforts have been undertaken to couple a CFD model to an HVAC or other building air quality model. Wang and Chen (2007) discuss that this coupling can take one of three basic forms: 1) The network model and the CFD model exchange pressures at common boundaries, 2) the network model exchanges pressure and the CFD model exchanges flow rate, and 3) the network model exchanges flow rate and the CFD model exchanges pressure.

In their effort, Wang and Chen coupled CONTAM to the CFD0 model. This effort was not focused on HVAC modeling so much as reducing the CFD expense to model room-to-room flows through open doors. They concluded that method 1) from above was the most stable approach. This method, however, is not easily implemented in the solution scheme used by FDS, whereas method 2) is. Other efforts to couple CFD models with network models have also

primarily focused on reducing the computation expense for modeling room to room flows rather than either HVAC functionality or fire effects [7]. The effort in this paper will focus on both HVAC functionality and fire effects.

This paper will describe the model equations, the solution method, and details of the coupling with the CFD solver. Verification of the model for some simple test cases will be demonstrated as well as comparisons of the model predictions for a series of tests involving a four level, twenty-three compartment building with three HVAC systems.

HVAC NETWORK MODEL

Overall Algorithm

The overall HVAC solver is based on the MELCOR (Gauntt, 2000) thermal hydraulic solver. MELCOR is a computer code for simulating accidents in nuclear power plant containment buildings. The Fire and Smoke Simulator (FSSIM) (Floyd, 2003), a network fire model, has shown prior success in using the MELCOR solver to model fire spread and smoke movement in the presence of complex ventilation systems.

The MELCOR solver uses an explicit conservation of mass and energy combined with an implicit solver for the conservation of momentum. An HVAC system is represented as network of nodes and ducts where a node represents where a duct joins with the FDS computational domain or where multiple ducts are joined such as a tee. A duct segment in the network represents any continuous flow path not interrupted by a node and as such may include multiple fittings (elbows, expansion or contractions, etc.) and may have varying area over its length. The current implementation of the model does not account for mass storage with an HVAC network. The conservation equations are:

Mass:

$$\sum_{j \text{ connected to } i} \rho_j u_j A_j = 0,$$

Energy:

$$\sum_{j \text{ connected to } i} \rho_j u_j A_j h_j = 0, \text{ and}$$

Momentum:

$$\rho_j L_j \frac{du_j}{dt} = (P_i - P_k) + (\rho g \Delta z)_j + \Delta P_j - \frac{1}{2} K_j \rho_j |u_j| u_j$$

Since nodes have no volume, the mass and energy conservation equations are merely that what flows into a node, must also flow out of the node. In the momentum equation the terms on the right hand side are: the pressure gradient between the upstream and the downstream node, the buoyancy head, pressure rise due to an external source (e.g. a fan or blower), and the pressure losses due to wall friction or the presence of duct fittings. The momentum equation is discretized in time which yields:

$$u_j^n = u_j^{n+1} \frac{\Delta t^n}{\rho_j L_j} \left((\tilde{P}_i^n - \tilde{P}_k^n) + (\rho g \Delta z)_j^{n-1} + \Delta P_j^{n-1} \right) - \frac{\Delta t^n K_j}{2L_j} \left(|u_j^{n-} - u_j^{n+}| u_j^{n-} - |u_j^{n+}| u_j^{n-} \right)$$

Note that the node pressures are not expressed as P_i^n , but rather as \tilde{P}_i^n . This indicates an extrapolated pressure at the end of the current time step rather than the actual pressure. The pressure in a compartment is a function of the mass and energy flows into and out of that compartment. If that compartment is connected to other compartments by doors or other openings, then the pressure is also dependent upon flows into and out those other compartments. Those mass and energy flows include both those being predicted by the HVAC model and those being predicted by the CFD model. For example, in Fig. 1, the un-shaded compartments have pressure solutions that are dependent upon the flows predicted by both the HVAC model and the CFD model and all of those compartments need to be included in the extrapolated pressure for those compartments.

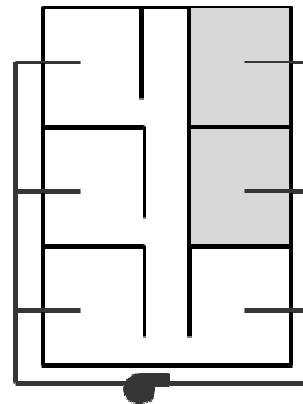


Figure 1: Example of pressure coupled (white) and uncoupled (gray) compartments.

Since the two models are not fully coupled, the extrapolated pressure is an estimate of the pressure at the end of the time step based upon the pressure rise for the prior time-step.

FDS decouples the pressure into a series of zone background pressures which vary with height but are otherwise constant in a pressure zone (a pressure zone is a region of the domain without a direct flow opening to another region such as a room with a closed door) and a dynamic pressure. The background pressure can change as a function of the mass and energy flows into or out of a pressure zone and is computed by summing the divergence inside of a pressure zone with the volume flows in and out of that pressure zone:

$$\frac{dP_m}{dt} = \left(\int_{\Omega_m} D dV - \int_{d\Omega_m} u \cdot dS \right) / \int_{\Omega_m} P dV$$

We can therefore estimate the extrapolated pressure at the next time step as:

$$\tilde{P}_m^n = P_m^{n-1} + \frac{dP_m^{n-1}}{dt} \Delta t^n$$

By removing the contribution of the prior time-step's HVAC contribution to the pressure rise, the extrapolated pressure can be expressed in terms of the HVAC solution for the current time step:

$$\begin{aligned} \tilde{P}_m^n &= P_m^{n-1} + \frac{dP_m^{n-1}}{dt} + \\ &\left(\sum_{j \text{ in } m} u_j^{n-1} A_j^{n-1} - \sum_{j \text{ in } m} u_j^n A_j^n \right) / \int_{\Omega_m} P dV = \\ &\tilde{P}_{m,non-hvac}^n - \sum_{j \text{ in } m} u_j^n A_j^n / \int_{\Omega_m} P dV \end{aligned}$$

Substituting into the velocity equation above:

$$\begin{aligned} &u_j^n \left(1 + \frac{K_j}{2L_j} |u_j^{n-} - u_j^{n+}| \right) - \\ &\frac{\Delta t^{n^2}}{\rho_j L_j} \left(\sum_{j \text{ in } i} u_j^n A_j^n / \int_{\Omega_i} P dV - \sum_{j \text{ in } k} u_j^n A_j^n / \int_{\Omega_k} P dV \right) \\ &= u_j^{n-1} + \\ &\frac{\Delta t^n}{\rho_j L_j} \left(\tilde{P}_{i,non-hvac}^n - \tilde{P}_{k,non-hvac}^n + (\rho g \Delta z)_j^{n-1} + \Delta P_j \right) \\ &+ \frac{K_j}{2L_j} |u_j^{n+}| |u_j^{n-}| \end{aligned}$$

The superscripts $n+$ and $n-$ on the velocity are used to linearize the flow loss in a duct to avoid a non-linear differential equation for velocity. The $n+$ superscript is the prior iteration value and the $n-$ is either the prior iteration value or zero if flow reversal occurred.

This approach, rather than $u_j^{n^2} \approx u_j^n u_j^{n-1}$, is used to speed convergence when duct flows are near zero to avoid large changes in K if the forward and reverse losses are marked different.

In the previous equation, if either duct node is an internal node (i.e. it is not connected to the domain the CFD model is solving for), then extrapolated pressure terms are not included for that node and the node pressure is solved for directly. For example if node i were an internal node, the equation would become:

$$\begin{aligned} &u_j^n \left(1 + \frac{K_j}{2L_j} |u_j^{n-} - u_j^{n+}| \right) - \\ &\frac{\Delta t^n}{\rho_j L_j} \left(P_i^n + \Delta t^n \sum_{j \text{ in } k} u_j^n A_j^n / \int_{\Omega_k} P dV \right) \\ &= u_j^{n-1} + \frac{\Delta t^n}{\rho_j L_j} \left(-\tilde{P}_{k,non-hvac}^n + (\rho g \Delta z)_j^{n-1} + \Delta P_j \right) \\ &+ \frac{K_j}{2L_j} |u_j^{n+}| |u_j^{n-}| \end{aligned}$$

The above equation for each duct along with a mass conservation equation for each internal duct node results in a set of linear equations for duct velocities and node pressures. The set of equations is solved, and the solution checked for error in mass conservation, flow reversal in a duct, and the magnitude change of the duct velocity from the prior iteration (or time step if the first iteration). If any convergence check fails, the solution is re-iterated.

Boundary Conditions of the HVAC Solver

The HVAC solver requires boundary conditions of pressure, temperature, and species for each duct node coupled to the CFD domain. For flows from a duct to the CFD domain, temperature and species are those of the duct. For flows from the CFD domain to a duct, the temperature and species are taken as the density weighted average of the gas cells adjacent to the vent coupling the CFD domain to the HVAC domain. Pressure is taken as the area weighted total pressure (background pressure plus dynamic pressure) over the vent. The total pressure is used so that the HVAC solver properly accounts for the direct impingement of fire driven flows onto a vent.

Boundary Conditions of the CFD Solver

The flows predicted by the HVAC solver are coupled to the CFD domain as vents of specified mass flux and temperature. The mass flux boundary condition is given by:

$$\dot{m}_{w,a}'' = Y_{j,a} u_j A_j \rho_j / A_{\text{CFD VENT}}$$

The wall temperature boundary condition is the duct temperature for flows into the CFD domain and the neighboring gas cell temperature for flows from the CFD domain. The boundary conditions for velocity, density, and species are given by:

$$\rho_w = \frac{\bar{W}_w P}{RT_w}; \quad \bar{W}_w = f(Y_w)$$
$$Y_{w,a} = \frac{\dot{m}_{w,a}'' + \frac{(\rho D)_w}{\Delta x_w} Y_{g,a}}{\frac{(\rho D)_w}{\Delta x_w} + u_w \rho_w}$$
$$u_w = \frac{a}{\rho_w A_w}$$

These variables are all coupled to one another; therefore, the solution is iterated. In most cases the boundary values change slowly from time step to time step and thus little iteration is required.

Limitations of the Current Implementation of the HVAC Solver

The current implementation of the HVAC solver has a number of limitations. These include:

- No reactions within the HVAC network (if hot unburned fuel from one room mixes with air from another room, it will not burn within the duct)
- No heat transfer from ducts to the FDS computational domain
- No mass storage in the HVAC network (what flows in also flows out in the same time step and there is no time delay in the transport of species through long ducts)
- Dampers are binary (fully open or fully closed)

All of the limitations above could be addressed by modifications to the solver.

Solution Scheme

The HVAC solution is updated in both the predictor and the corrector step of FDS. The sequence is as follows:

1. FDS updates the density solution.

2. At each HVAC node coupled to the FDS gas phase solution, determine the average temperature, pressure, density, and species.
3. Execute the HVAC solver.
4. Use the solution of the HVAC solver to update the FDS wall boundary conditions.
5. FDS continues on to its next step (updating the divergence).

VERIFICATION

Case 1 – Verify Flow Losses

In verification Case 1, a ceiling mounted supply duct is defined with an exit flow of 0.3 m³/s. Two floor mounted intake ducts, each with an area of 0.1 m², are connected via a tee to the exhaust duct. One leg of the tee (left vent in Fig. 2) is given a flow loss of 16 and the other a flow loss of 4 (right vent in Fig. 2). Since the two intakes are in the same compartment and have the same elevation, the pressure drop from intake to exhaust is the same in both cases. Therefore, the ratio of the duct velocities is given as the ratio of the square root of the flow losses, or 2:1. Figure 2 shows the results of this verification case. FDS predicts average duct velocities of 2.00 m/s and 1.00 m/s vs. the expected values of 2.00 m/s and 1.00 m/s. The fluctuations in duct velocity are expected and result from slight changes in the stagnation pressure at the inlets due to the time dependence of the flow in the FDS computational domain.

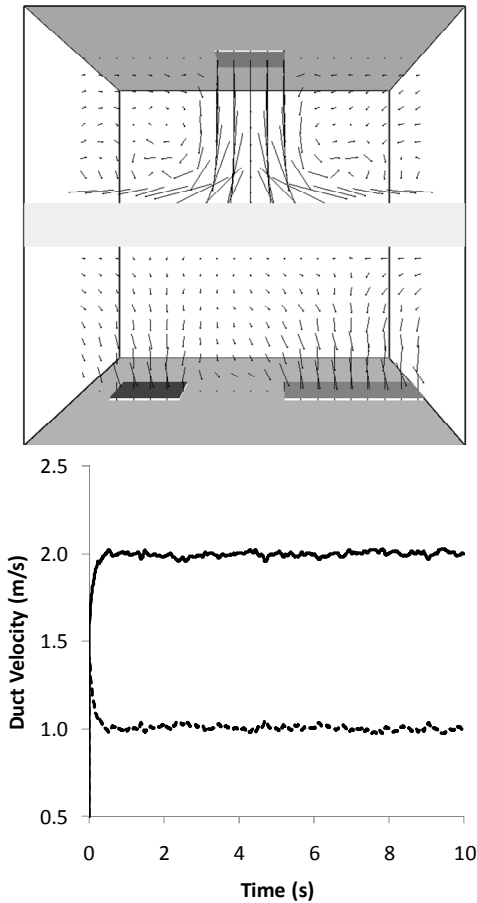


Figure 2: Results of verification Case 1.

Case 2 – Verify Species Conservation

In verification Case 2, a sealed compartment is initialized with another species in the bottom half of the compartment. This species is given the same molecular weight as air. Two ducts are specified with the same volume flow rate. One duct takes suction from the upper half of the compartment and discharges to the lower, and the other duct does the reverse. It is expected that for a brief period of time at the beginning of the simulation that the two outflow vents will show pure background species and pure other species until such time that the outflow plume reaches the intake. Figure 3 shows the results of this verification test. The image on the left is the species mass fraction at the beginning of the simulation and it shows (as expected) pure background species in the lower outflow and pure other species in the upper outflow. The middle image shows a short time later, when the outflow reaches its opposite intake. As expected, the outflow streams are now a mix of the two species. Plot on the right shows, as expected, that the total mass and the other species mass which does not change over time.

Case 3 – Verify Mass Conservation (Non-Uniform Temperature)

In verification Case 3, two equal compartments are separated by a vertical wall. One compartment is initialized to twice the absolute temperature as the other compartment. Two ducts of equal area, one at the top and one at the bottom, connect the two compartments. The bottom duct is given a specified volume flow of $0.1 \text{ m}^3/\text{s}$ from the hot compartment to the cold compartment. Similar to Case 2, we expect at the onset to see the hot compartment temperature in the outflow to the cold compartment and the cold compartment temperature in the outflow to the hot compartment until the outflow streams mix into the inlet flow. Figure 4 shows the results of the simulation where it is seen the behavior is as expected, that mass is conserved ($< 0.01\%$ mass error), and that equal velocities (and hence volume flow) are seen at steady state. The initial fluctuations in mass ($< 0.05\%$ of the total mass) result from numerical errors primarily due to the coarse grid used in the gas phase portion of the computation.

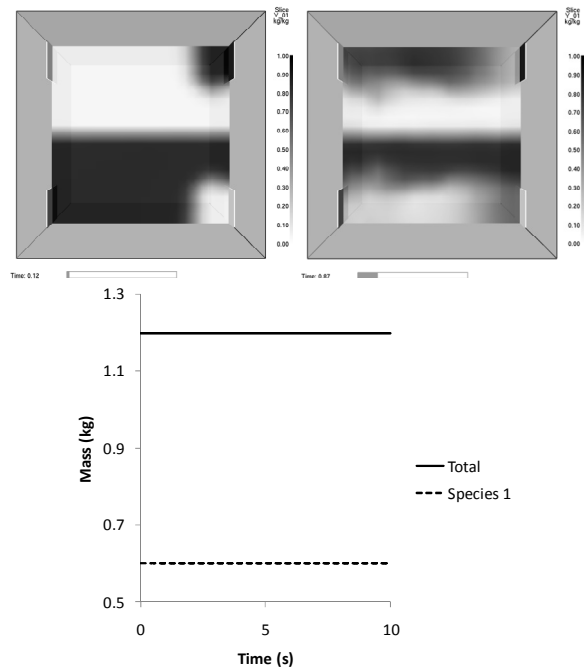


Figure 3: Results of verification Case 2.

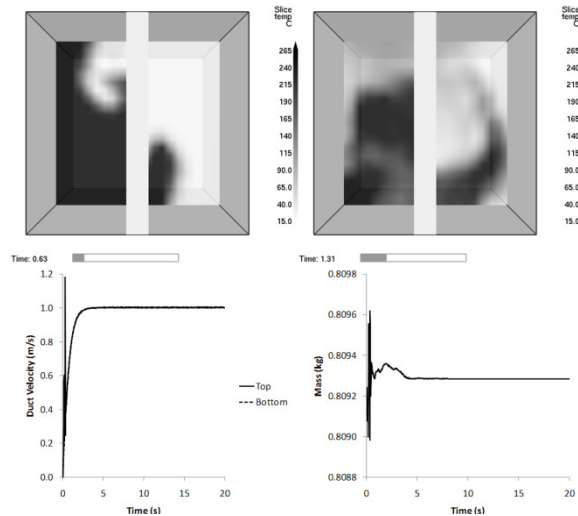


Figure 4: Results of verification Case 3.

VALIDATION

This section presents the results from two validation cases. One is a simple duct network solution from a handbook and the other is a complexly compartmented fire test facility.

Validation Case 1

The first validation case is example Problem #7 from the ASHRAE Fundamentals handbook (ASHRAE, 2007). This problem was designed to demonstrate how to perform a hand calculation to size a duct system to achieve desired flow rates. The HVAC system is depicted in Fig. 5, and it represents a metal working exhaust system where three pieces of equipment are exhausted through a cyclone dust collector. The numbered boxes indicate duct segments. Duct lengths, areas, and flow losses were specified in the example problem description. A quadratic fan curve was created that included the pressure vs. flow point determined in the ASHRAE solution. Table 1 compares the FDS predicted pressure drop over each duct segment with the pressure drop in the hand calculation. It is noted that the hand calculation assumes constant density, whereas the FDS calculation accounts for density changes that result from the pressure changes along the duct segments. Therefore, slight differences (on the order of a couple of Pascals) are expected in addition to any numerical error resulting from the HVAC solver.

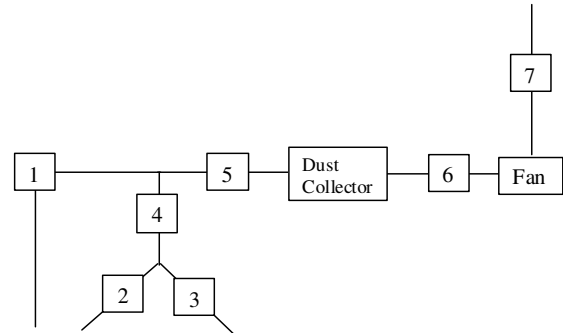


Figure 5: ASHRAE Problem #7 HVAC layout.

Table 1: FDS vs ASHRAE pressure drops

Segment	ASHRAE ΔP (Pa)	FDS ΔP (Pa)	Error (%)
1	739	731	1.1
2	457	449	1.8
3	283	282	0.4
4	124	124	0.0
5	748	744	0.5
6	33	33	0.0
7	324	321	0.9

Validation Cases 2 and 3 – Confined Space

Validation Cases 2 and 3 are fire tests in a confined space test facility (Floyd, 2005). The test facility consisted of 23 compartments over 4 levels with airtight external boundaries. 20 wall and ceiling openings were present in the facility. The facility contains three HVAC systems: a supply system which takes suction from a fan room and discharges to all compartments, an exhaust system which takes suction from all compartments and discharges to the fan room, and a smoke control system which takes suction from the L4-2 compartment and discharges it to the outside. The exhaust system had a second mode of operation where two dampers could be realigned to allow fresh air to be brought into the fan room while closing off the exhaust from the remainder of the facility. The facility is depicted in Fig. 6. For some tests two sets of four additional ducts were added. These ducts connected the ceiling of L2-1 to the floor of L4-1 with four ducts and the ceiling of L2-2 and the fire room to the floor of L4-2.

The HVAC systems were input based on as-built drawings and a walk down of the facility with loss coefficients developed using the ASHRAE Fundamentals handbook. Fan curves were taken from the manufacturer supplied data for the fans. Heat release rates were derived from load cell data for the weight of the fuel pan. Major sources of experimental uncertainty are the heat release rate, the soot yield (yield was estimated based on CO to CO₂ ratio), and

the actual vs. handbook flow losses in the HVAC system.

Two tests were simulated. The first test simulated was Test 4-10 which had a 1.05 m diesel pool fire, all the HVAC louvers blanked off (i.e. no-HVAC), no bypass ducts installed, no external closures opened, and all internal closures opened. The second test simulated was Test 5-14 which had a 0.68 m diesel pool fire, the bypass ducts installed, the external closure on Trunk 2 opened, most internal closures closed (many doors had ventilation grills in their lower third), and the supply and exhaust were run for one minute and then shut off and realigned for smoke control (exhaust bypass to the outside opened and the smoke control system on).

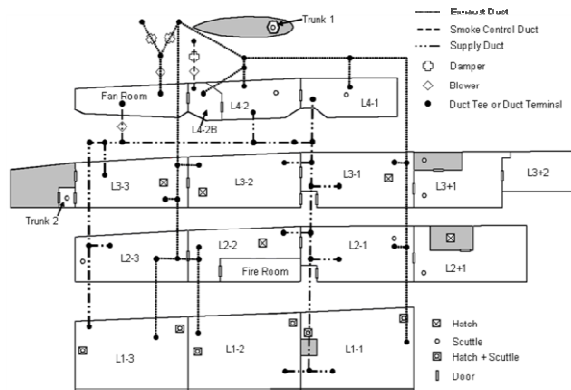
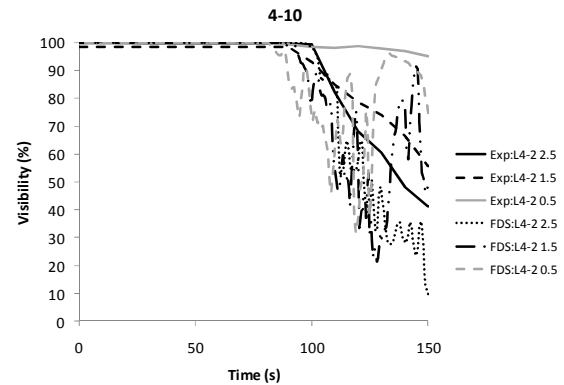


Figure 6: Confined space layout.

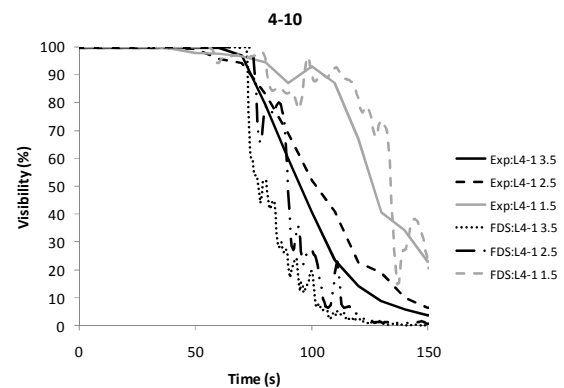
Figure 7 shows visibility measurements made in rooms 1 and 2 on the 4th level. In Test 4-10 with no HVAC present, FDS performs as expected. The delay time for smoke transport and the rates of decrease in visibility are well predicted (given the uncertainties in heat release rate, soot yield, and that soot deposition is not accounted for). In Test 5-14, FDS is predicting a shorter delay time than seen in the data, however, the current HVAC implementation does not account for transport delays which is contributing to this error. FDS predicts an equivalent overall rate of decrease in visibility.

Figure 8 shows velocities measured in doorways and floor openings. Figure 9 shows velocities measured in the HVAC system. These measurements were made with bi-directional probes. With the exception of the trunk inflow in Test 5-14, FDS predictions of door and floor opening velocities match the measured data. FDS predictions of flows in the mechanical HVAC systems agree with the measured data. Time to spin up and spin down the fans was not modeled in FDS which accounts for much of the difference in slope seen at one minute. A portion of the remaining error can be attributed to differences in the assumed duct losses (based on value in a handbook) vs. the actual duct losses and the actual fan performance vs.

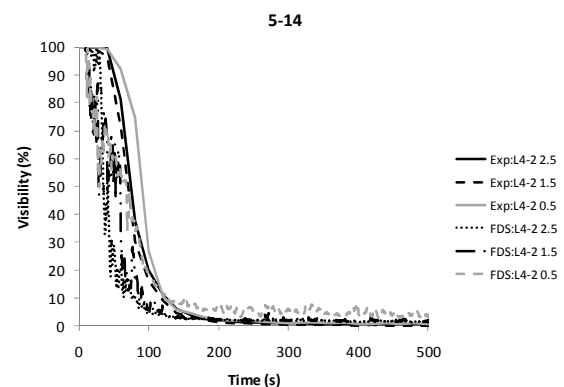
the manufacturer's data on fan performance. Given those uncertainties, the FDS predictions of duct velocities are excellent. Similarly the buoyancy driven flow through the bypass ducts are also well predicted. The largest prediction error is for the bypass ducts in the fire room and is likely a combination of errors in the loss specification, errors in the heat release specification, and overall predictive errors in FDS.



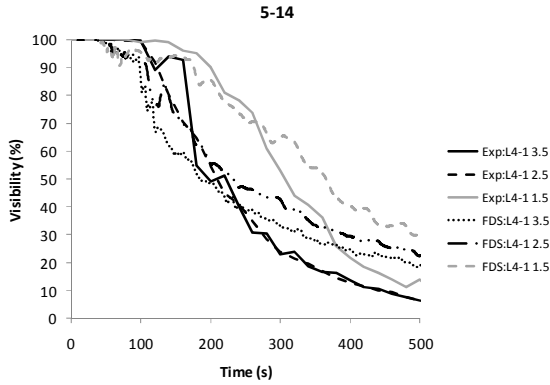
(a)



(b)

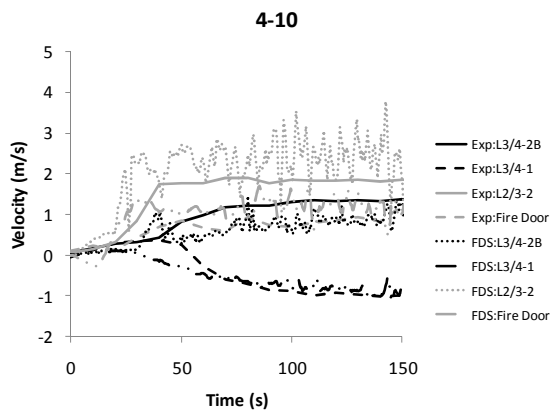


(c)

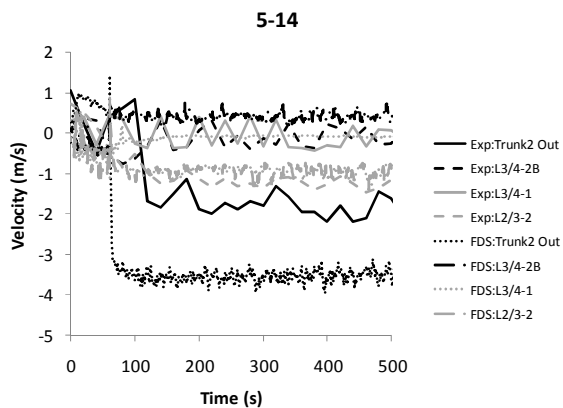


(d)

Figure 7: Level 4 visibility: (a) Test 4-10 compartment L4-2; (b) Test 4-10 compartment L4-1; (c) Test 5-14 compartment L4-2; (d) Test 5-14 compartment L4-1.

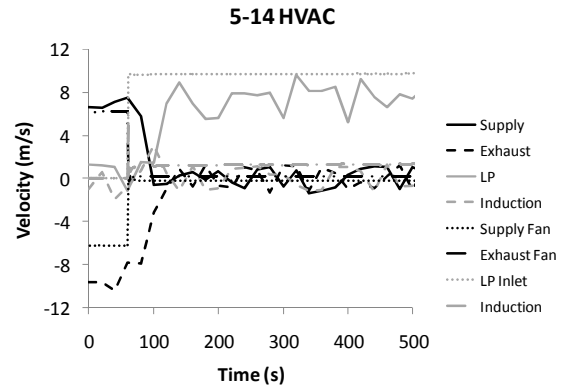


(a)

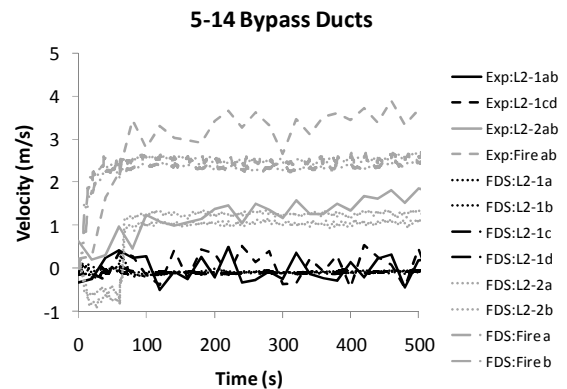


(b)

Figure 8: Door and floor opening velocities: (a) Test 4-10; (b) Test 5-14.



(a)



(b)

Figure 9: Duct velocities for test 5-14 (a) HVAC; (b) bypass ducts.

CONCLUSIONS

A network HVAC model based on the MELCOR algorithm has been coupled to FDS. The model includes fans, dampers, and forward and reverse flow losses. The model was coupled indirectly to FDS. The HVAC model uses prior time step gas cell values as the boundary conditions for the HVAC solver. The HVAC solution becomes the boundary condition for the current FDS time step. Since the pressure solutions are not directly coupled, some error will exist in the overall solution; however, since pressure typically changes slowly, this error is not likely to be large.

Verification of the HVAC model shows that the model properly accounts for flow losses in the input specifications. Verification also demonstrates that the model conserves mass for both isothermal and non-isothermal cases. Lastly the verification demonstrates that the use of FDS pressure zone data results in the correct HVAC system behavior.

Validation results were shown for a simple HVAC system that could be computed as a hand calculation as well as a complex set of HVAC systems that

change operational state over time in a confined space, multi-compartment facility with a fire. The simple system validation shows that the model correctly predicts pressure drops over a duct network. The confined space results show that the HVAC model allows for changes in operational state, correctly predicts HVAC duct flows for a complex network, and the coupling with FDS correctly captures buoyancy effects with the HVAC network.

FUTURE WORK

While the current HVAC implementation adds a tremendous amount of capability to FDS, there are a number of areas where additional work is needed:

- The HVAC solution is currently separate from the FDS leakage model which could result in stability issues in some circumstances. Since the leakage flow equation is similar to the momentum equation used in the HVAC model, the leakage solution should be merged in with the HVAC solution.
- Dampers are currently modeled as 100% open and 100% closed with instantaneous changes and similarly with fans. The process of opening and closing a damper or turning on and off a fan should include a brief transient period.
- There is currently no model for filtration (although a constant flow loss could be added to a duct to represent a filter). There are applications where loading of filters by soot is a concern and a filter model is desirable.
- Enthalpy additions or losses to duct flows are currently not modeled (e.g. heat transfer to duct walls or the presence of heat and cooling equipment).
- Expand the suite of verification and validation test cases.

NOMENCLATURE

A	area (m ²)
c_p	specific heat (J/kg/K)
E	energy (J)
g	gravity (9.80665 m/s ²)
h	enthalpy (J/kg)
K	loss coefficient (dimensionless)
L	length (m)
M, m	mass (kg)
P	pressure (Pa)
R	gas constant (8.314472 J/mol/K)
S	surface Area (m ²)
t	time (s)
Y	mass fraction (kg/kg)
u, \mathbf{u}	velocity (m/s)
V	volume (m ³)
W	molecular weight (kg/mol)

z elevation (m)

Greek

\mathcal{D} FDS divergence term

Ω computational mesh

ρ density (kg/m³)

subscripts

a species

g gas cell

i, k node

j duct

m pressure zone

w wall cell

superscripts

n current time-step

$n-1$ prior time-step

$n+$ prior iteration

$n-$ guess

\sim extrapolated value

REFERENCES

- American Society of Heating Refrigeration and Air-Conditioning Engineers, Inc. (2007), *ASHRAE Handbook Fundamentals*, ASHRAE, Atlanta, GA.
- Floyd, J., Hunt, S., Williams, F., and Tatem, P. (2004), Fire and Smoke Simulator (FSSIM) Version 1 – Theory Manual, Naval Research Laboratory NRL/MR/6180-04-8765, Washington, DC.
- Floyd, J., Hunt, S., Williams, F., and Tatem, P., (2005) “A Network Fire Model for the Simulation of Fire Growth and Smoke Spread in Multiple Compartments with Complex Ventilation”, *Journal of Fire Protection Engineering*, **15**(3),199-229, <http://dx.doi.org/10.1177/1042391505051358>.
- Gauntt, R. Cole, R., Erickson, R., Gido, R., Gasser, R., Rodriguez, S., Young, M., Ashbaugh, S., Leonard, M., Hill, A. (2000), MELCOR Computer Code Manuals: Reference Manuals Version 1.8.5, Volume 2, Rev. 2, US Nuclear Regulatory Commission NUREG/CR-6119. Washington, DC.
- Jones, W., Peacock, R., Forney, G. and Reneke, P. (2009), CFAST – Consolidated Model of Fire Growth and Smoke Transport (Version 6) Technical Reference Guide, National Institute of Standards and Technology NIST SP-1026, Gaithersburg, MD.
- McGrattan, K., Hostikka, S., Floyd, J., Baum, H., Rehm, R., Mell, W., and McDermott, R. (2010), “Fire Dynamics Simulator (Version 5) Technical Reference Guide, Volume 1: Mathematical

Model,” National Institute of Standards and Technology NIST SP-1018-5. Gaithersburg, MD.

Schaelin, A. and Dorer, V., (1993) Improvement of Multizone Model Predictions by Detailed Flow Path Values from CFD Calculation, *ASHRAE Transactions*, **105**(2), 414-427.

Walton, G. and Dols, W. (2008), CONTAM 2.4 User’s Guide and Program Documentation, National Institute of Standards and Technology NISTIR 7251, Gaithersburg, MD.

Wang, L., and Chen, Q.,(2007) “Theoretical and Numerical Studies of Coupling Multizone and CFD Models for Building Air Distribution Simulations”, *Indoor Air*, **17**, 348-361, <http://dx.doi.org/10.1111/j.1600-0668.2007.00481.x>.

Zhai, Z., Gao, Y. and Chen, Q. (2004), “Pressure Boundary Conditions in Multi-Zone and CFD Program Coupling”, *SimBuild 2004*, International Building Performance Simulation Association, Texas.